Iterative reconstruction and individualized automatic tube current selection reduce radiation dose while maintaining image quality in 320-multidetector computed tomography coronary angiography

Clinical Radiology 68 (2013) e570–e577

Contents lists available at SciVerse ScienceDirect

Clinical Radiology

journal homepage: www.clinicalradiologyonline.net

Iterative reconstruction and individualized automatic tube current selection reduce radiation dose while maintaining image quality in 320-multidetector computed tomography coronary angiography☆

M.C. Williams [a,*], N.W. Weir [b], S. Mirsadraee [b], F. Millar [a], A. Baird [b], F. Minns [b], N.G. Uren [c], G. McKillop [d], R.K. Bull [e], E.J.R. van Beek [b], J.H. Reid [b], D.E. Newby [a]

[a] *University of Edinburgh/British Heart Foundation Centre for Cardiovascular Science, Edinburgh, UK*
[b] *Clinical Research Imaging Centre, University of Edinburgh, UK*
[c] *Edinburgh Heart Centre, Royal Infirmary of Edinburgh, UK*
[d] *Department of Radiology, Royal Infirmary of Edinburgh, UK*
[e] *Royal Bournemouth Hospital, Castle Lane, East Bournemouth, UK*

ARTICLE INFORMATION

Article history:
Received 25 March 2013
Received in revised form
13 May 2013
Accepted 29 May 2013

AIM: To assess the effect of two iterative reconstruction algorithms (AIDR and AIDR3D) and individualized automatic tube current selection on radiation dose and image quality in computed tomography coronary angiography (CTCA).

MATERIALS AND METHODS: In a single-centre cohort study, 942 patients underwent electrocardiogram-gated CTCA using a 320-multidetector CT system. Images from group 1 ($n = 228$) were reconstructed with a filtered back projection algorithm (Quantum Denoising Software, QDS+). Iterative reconstruction was used for group 2 (AIDR, $n = 379$) and group 3 (AIDR3D, $n = 335$). Tube current was selected based on body mass index (BMI) for groups 1 and 2, and selected automatically based on scout image attenuation for group 3. Subjective image quality was graded on a four-point scale (1 = excellent, 4 = non-diagnostic).

RESULTS: There were no differences in age ($p = 0.975$), body mass index ($p = 0.435$), or heart rate ($p = 0.746$) between the groups. Image quality improved with iterative reconstruction and automatic tube current selection [1.3 (95% confidence intervals (CI): 1.2–1.4), 1.2 (1.1–1.2) and 1.1 (1–1.2) respectively; $p < 0.001$] and radiation dose decreased [274 (260–290), 242 (230–253) and 168 (156–180) mGy cm, respectively; $p < 0.001$].

CONCLUSION: The application of the latest iterative reconstruction algorithm and individualized automatic tube current selection can substantially reduce radiation dose whilst improving image quality in CTCA.

* Guarantor and correspondent: M.C. Williams, University of Edinburgh, British Heart Foundation Centre for Cardiovascular Science, Chancellor's Building, SU305, 49 Little France Crescent, EH16SU4 Scotland, UK. Tel.: +44 0131 242 6515, +44 07939511864; fax: +44 0131 242 6422.
E-mail address: michelle.williams@ed.ac.uk (M.C. Williams).

0009-9260/$ – see front matter © 2013 The Authors. Published by Elsevier Ltd on behalf of The Royal College of Radiologists. All rights reserved.
http://dx.doi.org/10.1016/j.crad.2013.05.098

Introduction

Computed tomography coronary angiography (CTCA) is a rapid minimally invasive test that is now widely used in the diagnosis of coronary artery disease, because diagnostic accuracy is comparable to invasive coronary angiography.[1] Radiation exposure is a major healthcare concern due to the increased lifetime risk of cancer,[2] and diagnostic cardiac imaging is responsible for 30% of radiation exposure.[3] Given that the use of CT is rapidly increasing,[4] it is important to develop strategies for CTCA that reduce radiation dose whilst maintaining image quality.

A variety of strategies to reduce radiation exposure in CTCA have been developed including prospective electrocardiogram gating, tube current modulation, tube voltage reduction, minimized scan range, and heart rate reduction.[5,6] Patient-tailored imaging is important to avoid under or over-exposure that can lead to grainy images or an unnecessarily high radiation dose. Patient-tailored imaging based on body mass index is widely used in CTCA.[7,8] However, body mass index is not necessarily an accurate guide to thoracic attenuation due to the wide variation in body habitus and fat distribution. Alternative methods proposed to select exposure settings include measurement of chest dimensions,[9] chest tissue composition,[10] scout image attenuation,[11] unenhanced attenuation,[12] and the use of automatic exposure control.[13]

Advances in CT technology have led to the development of iterative reconstruction techniques that have the potential to reduce radiation dose while maintaining image quality. Iterative reconstruction techniques were applied in early CT machines and have been widely used in nuclear medicine techniques, such as positron-emission tomography. However, the high computational demands and consequent long reconstruction times of iterative reconstruction algorithms meant that filtered back projection became more widely used in CT. More recently, iterative reconstruction algorithms have been shown to reduce image noise or radiation dose in CTCA.[14,15]

The combination of iterative reconstruction technology and individualized automatic tube current selection has the potential to reduce radiation dose whilst maintaining image quality. In the present study, the effect of applying iterative reconstruction and software that automatically selects tube current based on scout image attenuation, was assessed regarding radiation dose and image quality in CTCA.

Materials and methods

Study design

In a single-centre cohort study, the images of 942 consecutive patients who underwent clinically indicated CTCA using a 320-multidetector scanner (Aquilion ONE, Toshiba Medical Systems, Japan) were assessed. The local ethics committee waived the requirement for gaining informed consent for this study, as this was part of a clinical service development. Exclusion criteria for CT were documented severe allergy to iodinated contrast medium, impaired renal function (estimated glomerular filtration rate <30 ml/min), pregnancy, or weight exceeding the maximum tolerance of the CT bed (250 kg).

Patients were divided into three groups based on the reconstruction algorithm and method of tube current selection. Images from group 1 ($n = 228$) were reconstructed with a filtered back projection reconstruction algorithm (Quantum Denoising Software, QDS+). Iterative reconstruction was applied in group 2 [AIDR (Adaptive Iterative Dose Reduction), $n = 379$] and group 3 (AIDR3D, $n = 335$). Tube current was selected based on body mass index for group 1 and 2, but was selected automatically based on scout image attenuation for group 3.

Rate-limiting medication

Patients with a heart rate above 60 beats/min received rate-limiting medication with intravenous metoprolol (2.5–50 mg) or oral and intravenous verapamil (80 mg oral and 2.5–5 mg intravenous). All patients received sublingual glyceryl trinitrate (300 μg) unless contraindicated.

CT

After the acquisition of scout images, participants underwent prospective, electrocardiogram-gated contrast-enhanced CTCA using half-segment reconstruction and a 0.35 ms rotation time. Detector coverage was selected based on scout images to cover from 20 mm below the carina to the base of the heart using volume sizes of 160, 140, 128, 120, 100, or 80 mm. A tri-phasic injection of intravenous contrast agent (iomeprol, 400 mg iodine/ml; Iomeron 400, Bucks, UK) was administered based on body mass index (<30 kg/m^2, 50 ml; >30 kg/m^2, 60 ml, >40 kg/m^2, 70 ml).

Table 1
Selection of exposure settings for computed tomography coronary angiography.

Body mass index (kg/m^2)	Group 1 (QDS+)		Group 2 (AIDR)		Group 3 (AIDR3D and SUREexposure)	
	Tube voltage (kV)	Tube current (mA)	Tube voltage (kV)	Tube current (mA)	Tube voltage (kV)	Tube current (mA)
<20	100	400 to 450	100	320 to 360	100	Automatic selection based on scout image attenuation
20–26		450 to 580		360 to 460		
27–30	120	510 to 530	120	410 to 420	120	
31–38		560 to 570		450 to 460		
39–40	135	480 to 500		480 to 500		
>40		500	135	500		

Table 2
Patient characteristics.

	Group 1 (QDS+)	Group 2 (AIDR)	Group 3 (AIDR3D and SUREexposure)	*p*-Value
N	228	379	335	–
Age (years)	58 (56, 59)	58 (57, 59)	58 (57, 59)	0.975
Male	89 (39%)	182 (48%)	181 (54%)	0.002
Body mass index (kg/m^2)	29 (28, 30)	30 (29, 30)	29 (29, 30)	0.453
Heart rate (beats/min)	60 (58, 61)	60 (59, 61)	59 (58, 60)	0.746

Data are mean (95% confidence interval) or number (percentage).

For patients with a heart rate below 65 beats/min, images were acquired with an acquisition window of 70–80% of the interval between two consecutive QRS complexes. For patients with a heart rate above 65 beats/min the acquisition window was widened to 30–80%.

Tube voltage was selected based on body mass index. For groups 1 and 2, a tube voltage of 100 kV was used for patients with a body mass index <27 kg/m^2, 120 kV for 27–38 kg/m^2, and 135 kV $>$ 38 kg/m^2. For group 2, a tube voltage of 100 kV was used for patients with a body mass index ≤ 30 kg/m^2 and 120 kV for patients >30 kg/m^2. Tube current was selected based on body mass index for group 1 and group 2 (Table 1). For group 3 individualized, automated tube current selection based on scout image attenuation was applied (SUREexposure, Toshiba Medical Systems, Japan). The predetermined level of image noise was set at a standard deviation of 45 (0.5 mm section thickness, reconstruction kernel filter FC05). For groups 1 and 2, imaging was triggered when a threshold of 180 HU was reached in the left ventricle. For group 3, a more rapid triggering mechanism was used, where bolus triggering occurred during inspiration with reduced delay and a threshold of 340 HU in the left ventricle.

Image reconstruction

All images were reconstructed with a section thickness of 0.5 mm and an increment of 0.25 mm. Images from group 1 were reconstructed using the standard filtered back projection algorithm (QDS+) and a reconstruction kernel filter optimized for cardiac imaging (FC03). Images from group 2 were reconstructed using an iterative reconstruction algorithm (AIDR) and the same reconstruction kernel filter (FC03). Images from group 3 were reconstructed using a new iterative reconstruction algorithm (AIDR3D) with the standard level of blending. This produced visually softer images than QDS+ or AIDR algorithms, and thus, a slightly sharper reconstruction kernel filter (FC05) was used to obtain images that were subjectively assessed as similar between the three groups.

Radiation dose

The dose–length product displayed on the CT console after imaging was recorded. This was converted to millisieverts using the commonly used conversion factor of 0.014 mSv/mGy cm and an scanner-specific conversion factor of 0.028 mSv/mGy cm calculated using the method described by Huda et al.[16]

Image analysis

Images were analysed on a dedicated post-processing workstation (Vitrea fX, Vital Images, Minnetonka, MN, USA) and were assessed by two trained observers. Image quality was assessed on a four-point Likert scale (1 = excellent; 2 = mild reduction in image quality; 3 = moderate reduction in image quality; 4 = severe reduction in image quality).

Image noise was assessed with regions of interest placed in the ascending aorta at the level of the left main stem, the proximal interventricular septum, and in the liver. Image noise was determined as the standard deviations of the radiodensity within the region of interest. Contrast-to-noise ratio was calculated as the attenuation value in the aorta minus the attenuation value in the liver divided by the image noise in the aorta. The contrast-to-myocardium ratio was calculated as the attenuation value in the aorta minus the attenuation value in the interventricular septum divided by the image noise in the aorta.

Statistical analysis

Statistical analysis was performed using SPSS (version 18 for Mac OS X, IBM Armonk, NY, USA). Normally distributed quantitative variables are presented with mean and 95% confidence intervals. Non-normally distributed data are presented with median and interquartile ranges. Statistical significance was assessed using analysis of variance, Dunnett's *t*-test, or Pearson's chi-squared test as appropriate. A statistically significant difference was defined as a two-sided *p*-value <0.05.

Table 3
Details of computed tomography coronary angiography imaging.

		Group 1 (QDS+)	Group 2 (AIDR)	Group 3 (AIDR3D and SUREexposure)	*p*-Value
Scan range (mm)		133 (131, 134)	130 (129, 131)	128 (127, 129)	0.003
Acquisition window (30–80% versus 70–80%)		33/195	80/299	76/259	0.046
Contrast medium (ml)		55 (54, 56)	56 (55, 56)	55 (54, 56)	0.561
Tube voltage (kV)	100	34.2%	31.1%	57.3%	<0.001
	120	57.5%	59.6%	42.7%	
	135	8.3%	9.2%	0%	
Tube current (mA)	100 kV	538 (530, 547)	432 (425, 440)	334 (313, 355)	<0.001
	120 kV	538 (533, 543)	431 (428, 434)	426 (404, 448)	<0.001

Data are mean (95% confidence interval) or percentage (%).

Table 4
The effect of reconstruction on image quality and radiation dose.

	Group 1 (QDS+)	Group 2 (AIDR)	Group 3 (AIDR3D and SUREexposure)	*p*-Value
Subjective image quality	1.3 (1.2, 1.4)	1.2 (1.1, 1.2)[a]	1.1 (1.0-1.2)[a]	<0.001
Aorta attenuation (HU)	430 (416, 443)	426 (417, 434)	508 (495, 520)[a,b]	<0.001
Liver attenuation (HU)	65 (62, 68)	61 (59, 63)[a]	59 (58, 61)[a,b]	<0.001
IVS attenuation (HU)	89 (86, 92)	84 (83, 86)[a]	87 (85, 89)	0.007
Image noise aorta (HU)	32 (31, 33)	31 (30, 32)	41 (40, 41)[a,b]	<0.001
Image noise liver (HU)	39 (38, 41)	37 (36, 38)[a]	39 (39, 40)[b]	0.001
Image noise IVS (HU)	34 (33, 36)	31 (31, 32)[a]	37 (36, 37)[a,b]	<0.001
Contrast-to-noise ratio	12 (12, 13)	12 (12, 13)	11 (11, 12)[b,a]	0.005
Contrast-to-myocardium ratio	11 (11, 12)	11 (11, 12)	11 (10, 11)[b]	0.008
DLP (mGy cm)	274 (260, 290)	242 (230, 253)[a]	168 (156, 180)[a,b]	<0.001

Data are mean (95% confidence interval).
IVS, intraventricular septum; DLP, dose–length product; HU, Hounsfield unit.
[a] $p < 0.05$ compared to group 1.
[b] $p < 0.05$ compared to group 2.

Results

The images of 942 patients were assessed (group 1, $n = 228$; group 2, $n = 379$; group 3, $n = 335$). There were no differences in age, heart rate, or body mass index between the groups (Table 2). There was a small increase in the number of males imaged in groups 2 and 3. There was a small reduction in *z*-axis volume size and an increase in 30–80% acquisition windows between group 1 and groups 2 and 3 (Table 3). There was no difference in the volume of contrast medium used between groups.

There was an increase in the use of the lower tube voltage in group 3 ($p < 0.001$) and a reduction in tube current between group 1 and both groups 2 ($p < 0.001$) and 3 ($p < 0.001$; Table 2). The use of scout image-based selection of tube current led to the use of a much wider range of tube currents in group 3 (Fig 2).

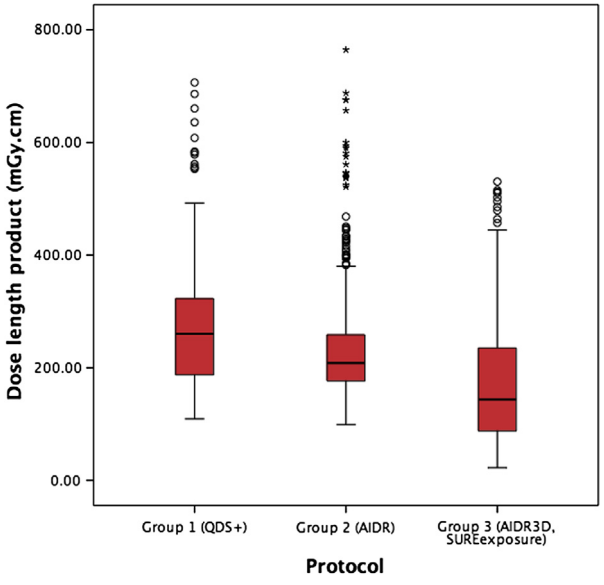

Figure 1 Box plot showing the reduction in the mean dose length product in groups 1, 2, and 3. There was a statistically significant reduction in dose–length product between groups 1 and 2, and groups 2 and 3.

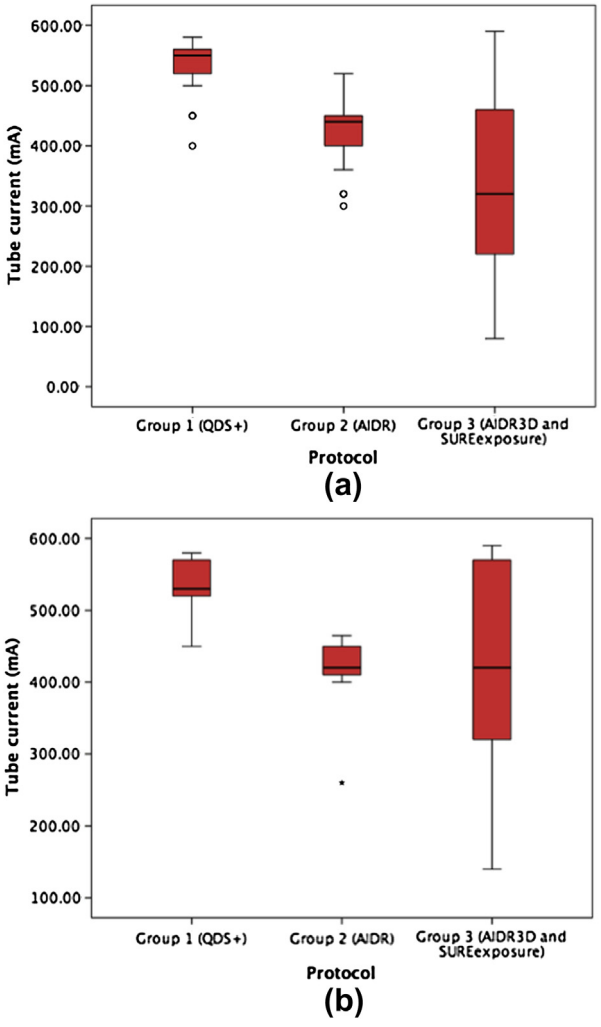

Figure 2 Box plots showing the reduction in the mean tube current between groups 1, 2, and 3 for patients imaged using (a) 100 kV and (b) 120 kV. There was a statistically significant reduction in tube current between groups 1 and 2, and groups 2 and 3. There was also an increase in the range of tube currents utilized in group 3.

Compared to filtered back projection (QDS+) reconstructions, the application of iterative reconstructions led to an improvement in subjective image quality ($p < 0.001$; Table 4). There was no difference in subjective image quality obtained between the two iterative reconstruction algorithms ($p = 0.861$). Figs 3–5 show example submillisievert images from patients in group 3 with normal, moderate, and severe coronary artery disease. Fig 6 shows coronary artery images from patients of all three groups with the same body mass index and sex.

For group 3, the attenuation density was higher in the aorta and lower in the liver (Table 4). However, there was no difference in attenuation density measured in the interventricular septum. There was an apparently small but not statistically significant reduction in noise between group 1 and group 2 in the liver and interventricular septum. There was an increase in noise in the aorta and interventricular septum in group 3. There was no difference in contrast-to-noise or contrast-to-myocardium between the three groups.

There was a reduction in radiation dose with the application of AIDR and AIDR3D protocols compared to the standard imaging protocol ($p = 0.001$ and $p < 0.001$, respectively; Table 4, Fig 1). Using the 0.014 mSv/mGy cm conversion factor, this equates to radiation exposures of 3.84 [95% confidence intervals (CI) CI: 3.64–4.06] mSv for group 1, 3.39 (CI: 3.22–3.54) mSv for group 2, and 2.35 (CI: 2.18–2.52) mSv for group 3. Using the 0.028 mSv/mGy cm conversion factor, this equates to radiation exposures of 7.67 (CI: 7.28–8.12) mSv for group 1, 6.78 (CI: 6.44–7.08) mSv for group 2, and 4.70 (CI: 4.37–5.04) mSv for group 3.

In addition, a post-hoc analysis was performed of 200 patients from each group matched for body mass index, sex, and acquisition window (see Supplementary material Table S1). The results were similar with a reduction in radiation dose [261 (CI: 246–276) mGy cm versus 211 (CI: 199–223) mGy cm versus 141 (CI: 129–153) mGy cm, $p < 0.001$], improvement in subjective image quality [1.3 (CI: 1.2–1.4) versus 1.1 (CI: 1.1–1.2) versus 1.1 (CI: 1.1–1.2); $p < 0.001$] and no difference in contrast-to-noise ratio between groups [12 (CI: 12–13) for all groups, $p = 0.747$)].

Thus compared to the standard imaging protocol, the application of AIDR and AIDR3D protocols led to a 12% and 39% reduction in radiation dose, respectively.

Discussion

The application of iterative reconstruction and automated selection of tube current based on the attenuation density of scout images can reduce radiation dose whilst maintaining image quality in CTCA. These adaptations are important given the widespread, escalating, and often repeated use of CTCA.

Iterative reconstruction algorithms have been shown to reduce image noise in CTCA. Tatsugami et al.[17] showed that reconstructing images using AIDR reduced image noise and contrast-to-noise ratio compared to the same data reconstructed with a filtered back projection algorithm. Similar results have been reported with other iterative reconstruction algorithms.[18,19] This decrease in image noise provides the potential to reduce tube current and voltage, and thus radiation dose, in CTCA. In a study of 70 patients, the application of AIDR, smaller scan ranges, and 100 kV tube voltage as part of a low-dose protocol led to an 80% reduction in radiation dose.[15] In the present study, a more modest reduction in radiation dose was observed but this reflected the fact that smaller scan ranges and 100 kV tube voltage had already been implemented where appropriate. Studies of other iterative reconstruction algorithms have identified radiation dose reductions of between 50 and 63%.[8,20,21] In a study of 243 patients imaged using the Adaptive Statistical Iterative Reconstruction (ASIR, GE Healthcare) algorithm compared to 331 patients using

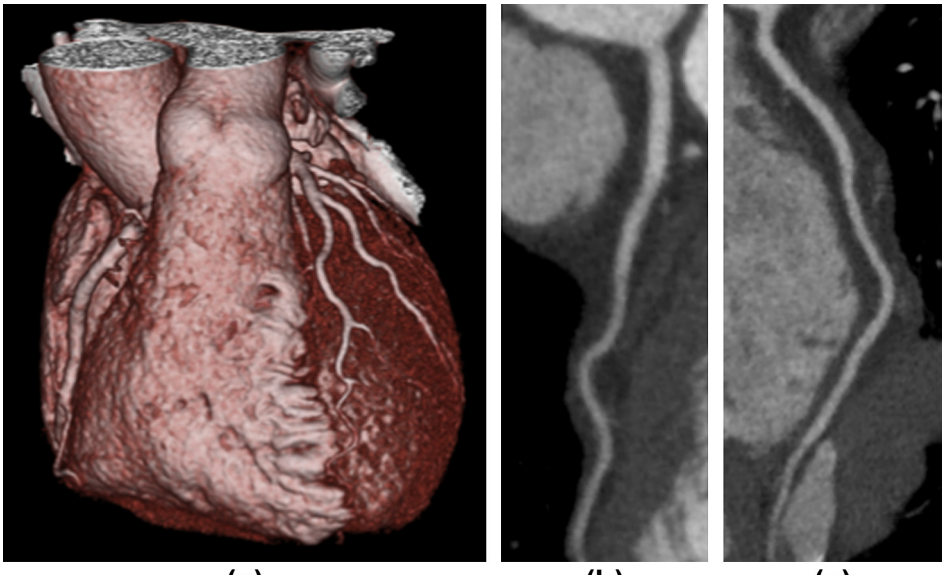

Figure 3 Example images from group 3 of a patient with normal coronary arteries showing (a) a three-dimensional (3D) image of the heart, (b) left anterior descending artery, and (c) right coronary artery. The female patient had a BMI of 20 and a radiation dose of 0.54 mSv (k = 0.014).

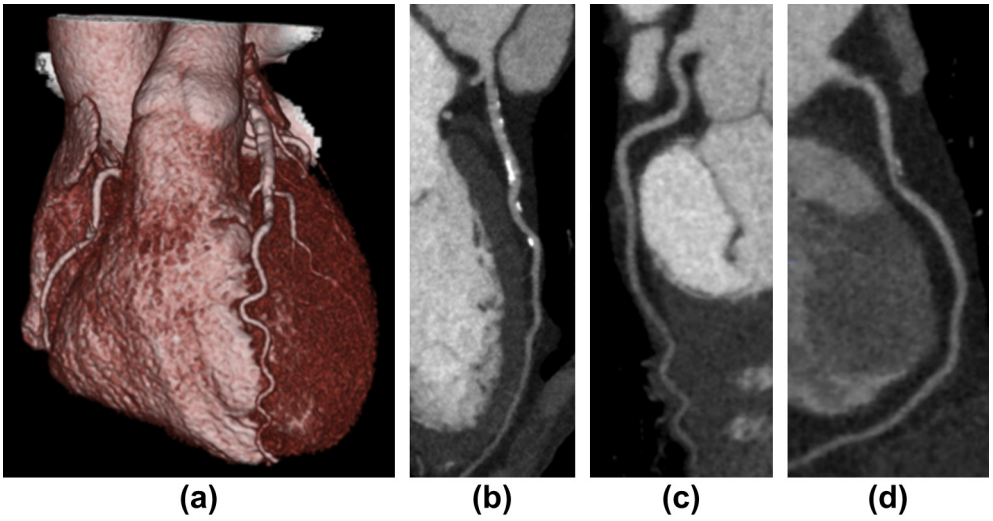

Figure 4 Example images from group 3 of a patient with moderate coronary artery disease showing (a) a 3D image of the heart, (b) the left anterior descending artery with areas of eccentric calcified plaque, (c) the normal left circumflex artery, and (d) the right coronary artery with mixed calcified and non-calcified plaque. The male patient had a BMI of 18 and a radiation dose of 0.66 mSv (k = 0.014).

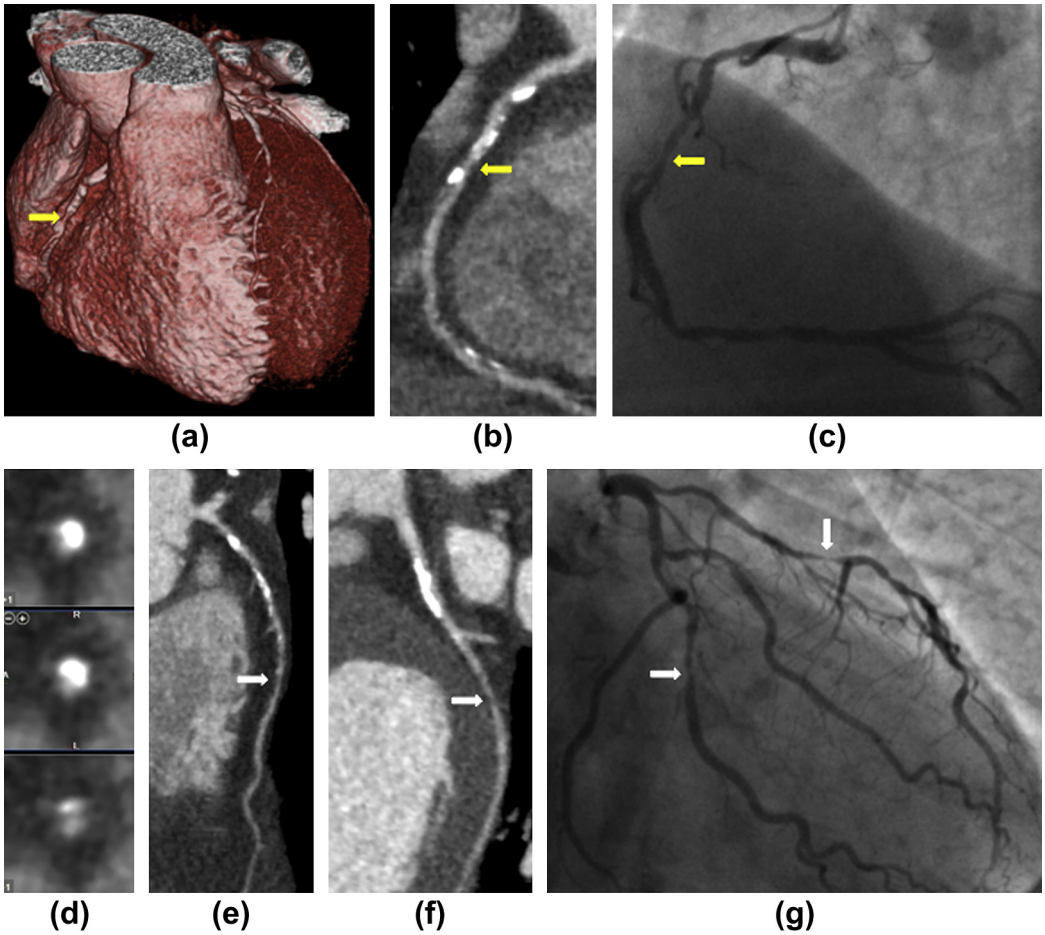

Figure 5 Example images from group 3 of a patient with severe three-vessel coronary artery disease. There was a severe stenosis of the right coronary artery (yellow arrows) identified on the 3D image of the heart (a), curved planar reformation (b), invasive coronary angiography (c), and cross-sectional images of the coronary artery (d) with areas of non-calcified plaque and both macro and microcalcifications. There were significant stenoses (white arrows) of the left anterior descending artery (e) and left circumflex artery (f) that corresponded to images obtained by invasive coronary angiography (g). The male patient had a BMI of 23 and a radiation dose of 0.86 mSv (k = 0.014).

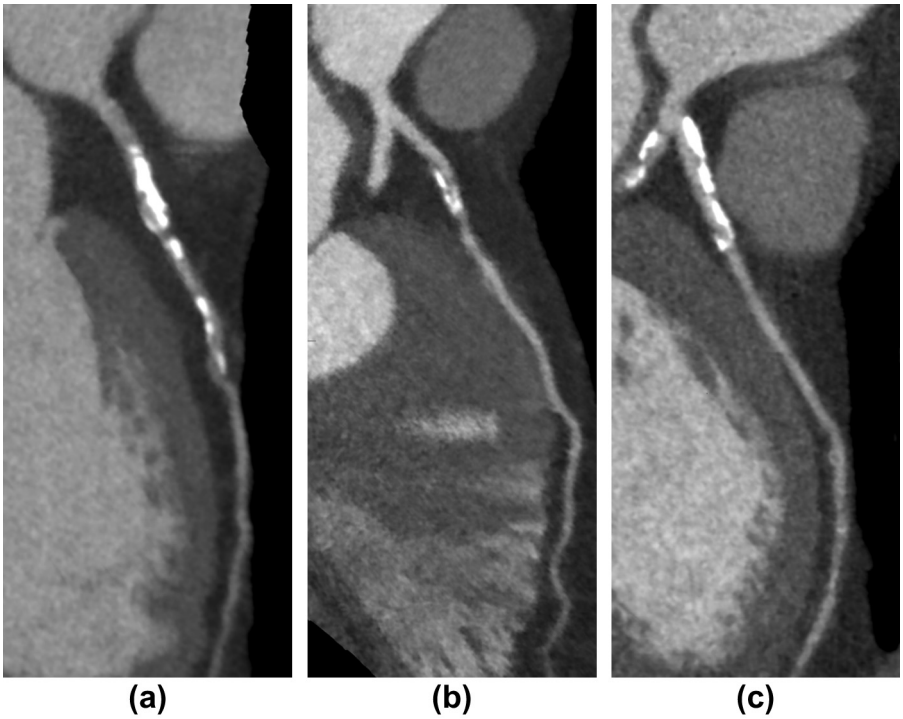

Figure 6 Example images from three patients with stenoses in their proximal left anterior descending arteries. The patients had the same body mass index (27 kg/m^2) and sex (male), and were from group 1 (a), group 2 (b), or group 3 (c).

filtered back projection, there was a 27% reduction in radiation dose when adjusted for imaging settings.[22] Similar to the present study, the reduction in radiation dose was due to the ability to reduce tube voltage and current. Although the lowest tube voltage used in the present study was 100 kV, the use of iterative reconstruction in combination with lower tube voltages, such as 80 kV, could further reduce radiation dose.[23]

The application of AIDR in the present study led to a reduction in image noise and maintenance of the contrast-to-noise ratio. However, the use of a different triggering mechanism and a different reconstruction kernel, in addition to the use of AIDR3D and SUREexposure, led to an increase in aorta contrast attenuation and image noise. Despite this, there was a small increase in subjective image quality in AIDR and AIDR3D groups. Iterative reconstruction algorithms may have effects in addition to alterations in image noise, as they have been shown to reduce the blooming artefact from calcified plaque[24] and other dense structures, such as coronary artery stents[25] and mechanical prosthetic heart valves.[26]

Both body mass index and scout image attenuation were used to tailor images to the individual patient. The use of chest tissue attenuation to select exposure settings reduces radiation dose in CTCA[11,12] and coronary artery calcium scoring.[27] These previous studies used manual measurements and calculations, whereas the automated method applied in the present study was rapid and easy to use. Patient-tailored imaging is important in order to follow the ALARA (As Low As Reasonably Achievable) principle. This is particularly important for young women who are at the greatest lifetime risk of developing cancer.[2] Patient-tailored imaging also enables the maintenance of more consistent image quality: an important consideration as image quality is associated with diagnostic accuracy.[28]

Study limitations

This was an observational cohort study as the nature of the software changes between reconstruction algorithms, which precluded a randomized study. Differences in software may have contributed to the results of the study outwith the effect of iterative reconstruction. For example, scanner software versions 4.4, 4.5, or 4.6 were applied for group 1, version 4.6 for group 2, and version 4.7 for group 3. These data were collected over a prolonged period of time, and thus, changes in referral patterns led to a difference in sex frequencies between the groups. Men tend to have larger coronary arteries and better image quality at CTCA.[29] Thus, that some of the observed benefit in image quality may be attributable to this cannot be excluded. The difference in the scan range between groups may also have contributed to the results. However, in the post-hoc analysis, the results were similar and there was no difference in scan range.

Diagnostic accuracy in comparison to invasive coronary angiography was not assessed. The iterative reconstruction algorithm produces smoother images, and thus, there is the possibility that the degree of stenosis could be misinterpreted, particularly in smaller vessels, heavily calcified vessels, or coronary artery stents. In addition, the use of lower tube voltages, such as 80 kV, may not produce images that are diagnostically similar to 100 or 120 kV. In striving to

reduce radiation dose, it is important that image quality and diagnostic accuracy are not compromised. Evidence of harm from radiation exposure at these levels is extrapolated and remains controversial. In addition, iterative reconstruction should not be applied as an alternative to good practice in applying optimized protocols.

A further limitation is that image quality was assessed on a per-patient rather than a per-segment level. It was more clinically relevant to assess image quality per patient, as this most directly influences future investigations or treatment. It was not possible to blind observers to the reconstruction technique as, although reconstruction kernel filters were chosen to produce similar results, it is possible to differentiate between the images based on subtle differences.

In conclusion, CTCA is an increasing source of population radiation exposure and this can be dramatically reduced by the application of patient-tailored imaging protocols and iterative reconstruction. These approaches should now be routinely used in clinical practice to minimize the harm of this extremely valuable and emerging diagnostic imaging technology.

Acknowledgements

M.C.W. is supported by a British Heart Foundation Clinical Research and Training Fellowship (FS/11/14/28692) and D.E.N. holds the British Heart Foundation John Wheatley Chair of Cardiology (CH/09/002). E.J.R.V.B. is the Scottish Imaging Network A Platform of Scientific Excellence Chair of Clinical Radiology. Some imaging was funded by the Chief Scientist Office, Scottish Government (CZH/4/588), UK. The Centre for Cardiovascular Science is the recipient of a British Heart Foundation Centre of Research Excellence Award (RE/08/001). The Clinical Research Imaging Centre is supported by NHS Research Scotland (NRS) through NHS Lothian. M.C.W., D.E.N., and E.J.R.V.B. have spoken at meetings sponsored by Toshiba Medical Systems.

Appendix A. Supplementary material

Supplementary material related to this article can be found online at http://dx.doi.org/10.1016/j.crad.2013.05.098.

References

1. Miller JM, Rochitte CE, Dewey M, et al. Diagnostic performance of coronary angiography by 64-row CT. *N Engl J Med* 2008;**359**:2324–36.
2. Einstein AJ, Henzlova MJ, Rajagopalan S. Estimating risk of cancer associated with radiation exposure from 64-slice computed tomography coronary angiography. *JAMA* 2007;**298**:317–23.
3. Fazel R, Krumholz HM, Wang Y, et al. Exposure to low-dose ionizing radiation from medical imaging procedures. *N Engl J Med* 2009;**361**:849–57.
4. Brenner DJ, Hall EJ. Computed tomography—an increasing source of radiation exposure. *N Engl J Med* 2007;**357**:2277–84.
5. Raff GL, Chinnaiyan KM, Share D, et al. Radiation dose from cardiac computed tomography before and after implementation of radiation dose-reduction techniques. *JAMA* 2009;**301**:2340–8.
6. Labounty TM, Earls JP, Leipsic J, et al. Effect of a standardized quality-improvement protocol on radiation dose in coronary computed tomographic angiography. *Am J Cardiol* 2010;**106**:1663–7.
7. Alkadhi H, Stolzmann P, Scheffel H, et al. Radiation dose of cardiac dual-source CT: the effect of tailoring the protocol to patient-specific parameters. *Eur J Radiol* 2008;**68**:385–91.
8. Hosch W, Stiller W, Mueller D, et al. Reduction of radiation exposure and improvement of image quality with BMI-adapted prospective cardiac computed tomography and iterative reconstruction. *Eur J Radiol* 2011;**81**:3568–76.
9. Rogalla P, Blobel J, Kandel S, et al. Radiation dose optimisation in dynamic volume CT of the heart: tube current adaptation based on anterior–posterior chest diameter. *Int J Cardiovasc Imaging* 2010;**26**:933–40.
10. Paul NS, Kashani H, Odedra D, et al. The influence of chest wall tissue composition in determining image noise during cardiac CT. *AJR Am J Roentgenol* 2011;**197**:1328–34.
11. Gao J, Li J, Earls J, et al. Individualized tube current selection for 64-row cardiac CTA based on analysis of the scout view. *Eur J Radiol* 2010;**79**:266–71.
12. Paul J- F. Individually adapted coronary 64-slice CT angiography based on precontrast attenuation values, using different kVp and tube current settings: evaluation of image quality. *Int J Cardiovasc Imaging* 2011;**27**:53–9.
13. Deetjen A, Möllmann S, Conradi G, et al. Use of automatic exposure control in multislice computed tomography of the coronaries: comparison of 16-slice and 64-slice scanner data with conventional coronary angiography. *Heart* 2007;**93**:1040–3.
14. Gervaise A, Osemont B, Lecocq S, et al. CT image quality improvement using Adaptive Iterative Dose Reduction with wide-volume acquisition on 320-detector CT. *Eur Radiol* 2012;**22**:295–301.
15. Gagarina NV, Irwan R, Gordina G, et al. Image quality in reduced-dose coronary CT angiography. *Acad Radiol* 2011;**18**:984–90.
16. Huda W, Tipnis S, Sterzik A, et al. Computing effective dose in cardiac CT. *Phys Med Biol* 2010;**55**:3675–84.
17. Tatsugami F, Matsuki M, Nakai G, et al. The effect of adaptive iterative dose reduction on image quality in 320-detector row CT coronary angiography. *Br J Radiol* 2012;**85**:e378–82.
18. Bittencourt MS, Schmidt B, Seltmann M, et al. Iterative reconstruction in image space (IRIS) in cardiac computed tomography: initial experience. *Int J Cardiovasc Imaging* 2010;**27**:1081–7.
19. Leipsic J, Labounty TM, Heilbron B, et al. Adaptive statistical iterative reconstruction: assessment of image noise and image quality in coronary CT angiography. *AJR Am J Roentgenol* 2010;**195**:649–54.
20. Wang R, Schoepf UJ, Wu R, et al. Image quality and radiation dose of low dose coronary CT angiography in obese patients: sinogram affirmed iterative reconstruction versus filtered back projection. *Eur J Radiol* 2012;**81**:3141–5.
21. Park E-A, Lee W, Kim KW, et al. Iterative reconstruction of dual-source coronary CT angiography: assessment of image quality and radiation dose. *Int J Cardiovasc Imaging* 2011;**28**:1775–86.
22. Leipsic J, Labounty TM, Heilbron B, et al. Estimated radiation dose reduction using adaptive statistical iterative reconstruction in coronary CT angiography: the ERASIR study. *Am J Roentgenol* 2010;**195**:655–60.
23. Oda S, Utsunomiya D, Funama Y, et al. A hybrid iterative reconstruction algorithm that improves the image quality of low-tube-voltage coronary CT angiography. *AJR Am J Roentgenol* 2012;**198**:1126–31.
24. Renker M, Nance JW, Schoepf UJ, et al. Evaluation of heavily calcified vessels with coronary CT angiography: comparison of iterative and filtered back projection. *Radiology* 2011;**260**:390–9.
25. Ebersberger U, Tricarico F, Schoepf UJ, et al. CT evaluation of coronary artery stents with iterative image reconstruction: improvements in image quality and potential for radiation dose reduction. *Eur Radiol* 2012;**31**:125–32.
26. Habets J, Symersky P, de Mol BA, et al. A novel iterative reconstruction algorithm allows reduced dose multidetector-row CT imaging of mechanical prosthetic heart valves. *Int J Cardiovasc Imaging* 2011;**28**:1567–75.
27. Horiguchi J, Matsuura N, Yamamoto H, et al. Evaluation of attenuation-based tube current control in coronary artery calcium scoring on prospective ECG-triggered 64-detector CT. *Acad Radiol* 2009;**16**:1231–40.
28. Dewey M, Vavere AL, Arbab-Zadeh A, et al. Patient characteristics as predictors of image quality and diagnostic accuracy of MDCT compared with conventional coronary angiography for detecting coronary artery stenoses: CORE-64 Multicenter International Trial. *Am J Roentgenol* 2010;**194**:93–102.
29. Dewey M, Rutsch W, Hamm B. Is there a gender difference in noninvasive coronary imaging? Multislice computed tomography for noninvasive detection of coronary stenoses. *BMC Cardiovasc Disord* 2008;**8**:2.